CALIBRATION AND VALIDATION OF A DRUCKER–PRAGER CAP MODEL FOR SIMULATING TILE BODY FORMING

J.M. Tiscar[(1)]; J. Balaguer[(1)]; M. Soriano[(1)]; M.J. Sánchez[(1)], J.A. Pérez[(2)] F.A. Gilabert[(3)]

(1) Instituto de Tecnología Cerámica (ITC). Asociación de Investigación de las Industrias Cerámicas (AICE). Universitat Jaume I. Castellón. Spain.
(2) MACER, S.L.
(3) Department of Materials, Textiles and Chemical Engineering (MaTCh), Mechanics of Materials and Structures. Ghent University (UGent). Ghent. Belgium.

ABSTRACT

The forming of ceramic tiles is a complex process in which a bed of powder is transformed into a rigid, continuous material. During this process, the properties of the powder undergo changes as compaction pressure increases, decreasing porosity until it reaches a minimum value, which depends on various factors such as the pressure applied, moisture content and initial porosity, among others.

The forming process has advanced to the point where tiles with pronounced reliefs and large ceramic slabs can be formed. However, these advances in the manufacture of ceramic bodies have entailed major technical challenges. Indeed, a significant increase has arisen in the occurrence of defects, including crack formation, excessive deformations and heterogeneous bulk density distributions in tiles or slabs. These defects compromise the structural integrity of the ceramic bodies, generating premature failure and impacting the durability of the product. Therefore, accurate and validated numerical models are essential to predict and optimise the forming process.

This paper proposes to calibrate the Drucker–Prager Cap (DPC) elasto-plastic model for use in simulating the tile forming process, using solid mechanics and the finite element method (FEM). This model is an extension of the Drucker–Prager yield model, widely used in the study of geological materials that exhibit pressure-dependent yield behaviour.

1. INTRODUCTION

The process of forming ceramic tile bodies represents a major manufacturing challenge, combining science and technology to transform a bed of powder into a solid, continuous material. In this process, the powder undergoes a transformation in which its properties change dramatically as compaction pressure increases and bed porosity decreases to a minimum value. Unfired body porosity, crucial in defining end product quality, depends on several factors, such as the maximum pressure applied, moisture content of the pressed powder, and particle size distribution in the powder, among others.

Body forming has historically been performed using the semi-dry uniaxial pressing technique, which involves the use of highly flowable granular powder and hydraulic presses equipped with metal dies. While effective, industry demands in recent years have led the method to be partially replaced by continuous compactors, which have made it possible to manufacture large-sized ceramic slabs, with widths up to 2000 mm and lengths of over 3000 mm [1]. Furthermore, the constant evolution of the ceramic tile industry has also enabled three-dimensional pieces with very pronounced reliefs to be produced.

Such advances in ceramic body manufacturing have brought with them a number of significant technical challenges. In particular, a notable increase has been seen in the appearance of defects, cracks, excessive deformations and heterogeneous bulk density distributions in tiles or slabs. These defects can compromise the structural integrity of ceramic bodies, affecting the durability of the end product. Given this context, it is essential that accurate and validated numerical models to predict material behaviour be made available in order to anticipate and optimise the forming process.

This study proposes an innovative approach to model the ceramic tile forming process. The approach is based on applying solid mechanics principles and using the finite element method (FEM). A key part of such a process is the implementation of a model that describes the elasto-plastic behaviour of the powder bed during forming. One of the most widely used models in powder forming is the elasto-plastic Drucker–Prager Cap (DPC) model, an extension of the Drucker–Prager yield model. Although originally developed for the study of geological materials with pressure-dependent yield behaviour [2,3], the DPC model has the necessary characteristics to adequately describe the behaviour of the powder bed and possible fracture of the material during ceramic forming.

The main objective of this research focuses on the calibration and validation of the DPC model applied to the forming of porcelain stoneware tile bodies. Such a task involves collecting experimental data obtained from laboratory tests specifically designed to describe the behaviour of porcelain stoneware tile powder beds. Through this calibration process, the parameters of the DPC model can be adjusted to achieve an accurate match of the numerical results and the experimental data.

Once the calibration and validation processes have been successfully completed, the model can be used to accurately predict material behaviour during the forming of ceramic bodies under a wide variety of conditions. In addition, it allows process parameters to be optimised [4], which significantly contributes to improving the efficiency and quality of tile body manufacturing.

2. OBJECTIVE

The main aim of this work is to calibrate a DPC elasto-plastic model for application in the modelling of the ceramic tile forming stage. The ultimate goal is to predict powder bed deformation during forming, the stress state and bulk density distribution in the material after pressing.

3. DRUCKER–PRAGER CAP BEHAVIOUR MODEL

The material model used in this study is a modified version of the DPC model, as proposed by several authors [5,6]. This model is by far the most widely used to describe the mechanical behaviour of powder during the compaction process of a powder bed [7]–[10], as it accurately describes the stress, displacement and density distributions within the bed during the forming process. As a starting point, the version implemented in the ABAQUS® commercial software was used. That version was modified by defining the model parameters as a function of volumetric plastic deformation, which in turn may be related to the density of the material. The modification was introduced through a user subroutine (USDFLD) available in ABAQUS® to formulate solution-dependent parameters.

As figure 1 shows, the DPC yield surface is bounded by three surfaces: a conical shear surface (present in the classical form of the Drucker–Prager yield criterion), an elliptical surface (called the "cap"), and a transition surface between the two, to establish a smooth transition and avoid numerical instabilities.

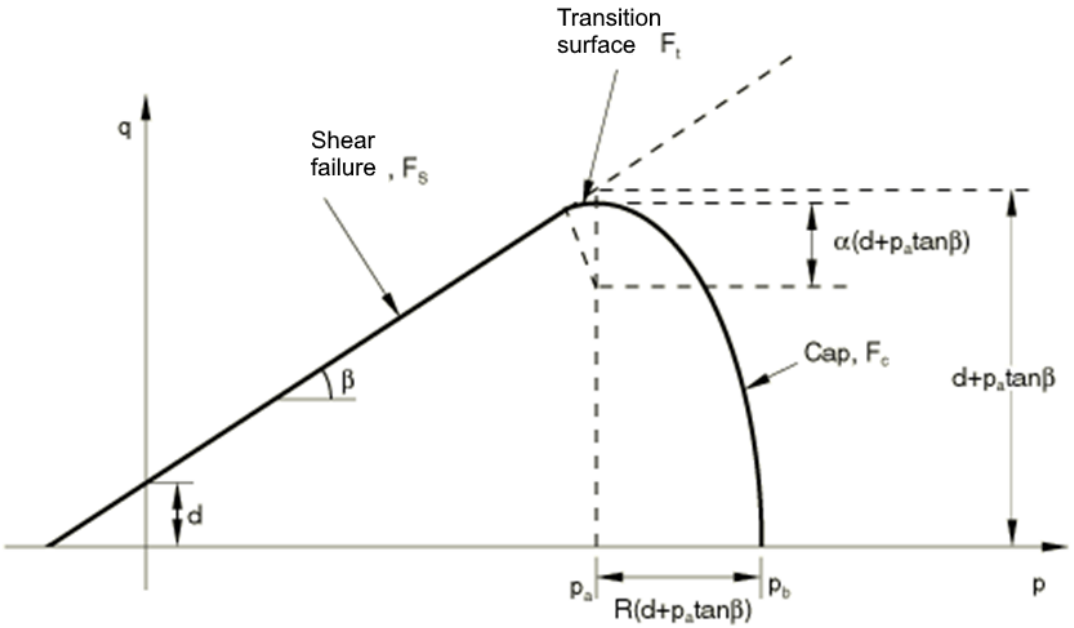

***Figure 1**. p-q diagram of the modified Drucker–Prager Cap model*

Consequently, the yield condition consists of the three separate equations shown below: Fs(p,q), F_C(p,q) and F_T(p,q) (in which the subscript letters refer to shear surface, cap surface and transition surface, respectively):

$$F_s(p,q) = q - \tan(\beta)p - d = 0 \quad (1)$$

$$F_C(p,q) = \sqrt{(p-p_a)^2 + \left[\frac{R \cdot q}{1+\alpha-\alpha/\cos\beta}\right]^2} - R(d + p_a \tan\beta) = 0 \quad (2)$$

$$F_T(p,q) = \sqrt{(p-p_a)^2 + \left[q - \left(1 - \frac{\alpha}{\cos\beta}\right)(d + p_a \tan\beta)\right]^2} - \alpha(d + p_a \tan\beta) = 0 \quad (3)$$

where p and q are the hydrostatic pressure and Von Mises equivalent stress, respectively. In addition, the model available in ABAQUS® applies a plastic flow rule associated with the cap surface (G_c) and a non-associated flow rule (G_s) in the shear surface and in the transition surface defined by equations (4) and (5).

$$G_C(\sigma) = \sqrt{(p-p_a)^2 + \left[\frac{R \cdot q}{1+\alpha-\alpha/\cos\beta}\right]^2} \quad (4)$$

$$G_S(\sigma) = \sqrt{[(p-p_a)\tan\beta]^2 + \left[\frac{q}{1+\alpha-\alpha/\cos\beta}\right]^2} \quad (5)$$

Thus, the DPC model is fully defined by determining the five constitutive parameters used in the yield condition given by (1)–(3): material cohesion ***d*** and friction angle ***β*** required to define the shear surface, "cap" eccentricity ***R,*** and evolution pressure $\boldsymbol{p_a}$ (or, alternatively, the hydrostatic yield pressure $\boldsymbol{p_b}$); see figure 1 to define the shape and position of the cap and parameter ***α*** that governs the transition region (i.e. the connection between the cap and the shear failure surface).

Model modification consists of implementing the evolution of the parameters during the compaction process. This change in the plastic parameters during plastic deformation is called "hardening", which in this particular study is directly linked to the bulk density of the material.

In turn, bulk density is related to an internal variable, common to any elasto-plastic model, called volumetric plastic deformation, ε_p^V (plastic deformation that implies a change of volume in the material). Therefore, it is possible to relate the bulk density of the material to the ε_p^V by means of the following expression:

$$\varepsilon_p^V = \ln\frac{\rho}{\rho_0} \quad (6)$$

where ρ and ρ_0 represent current and initial bulk density (corresponding to a volumetric plastic deformation of 0), respectively.

4. EXPERIMENTAL PROCEDURE

The experimental procedure carried out to obtain the physical properties of a powder bed in its forming process, as well as the equipment and materials used, are described below.

4.1. MATERIALS AND EQUIPMENT

The following materials and equipment were used to calibrate the model.

4.1.1. POWDER MATERIAL

A standard spray-dried powder used in the manufacture of porcelain stoneware tile was employed as the powder material. Powder moisture content on a dry basis during its characterisation was 6.5%. Figure 2 shows the size distribution of the powder granules.

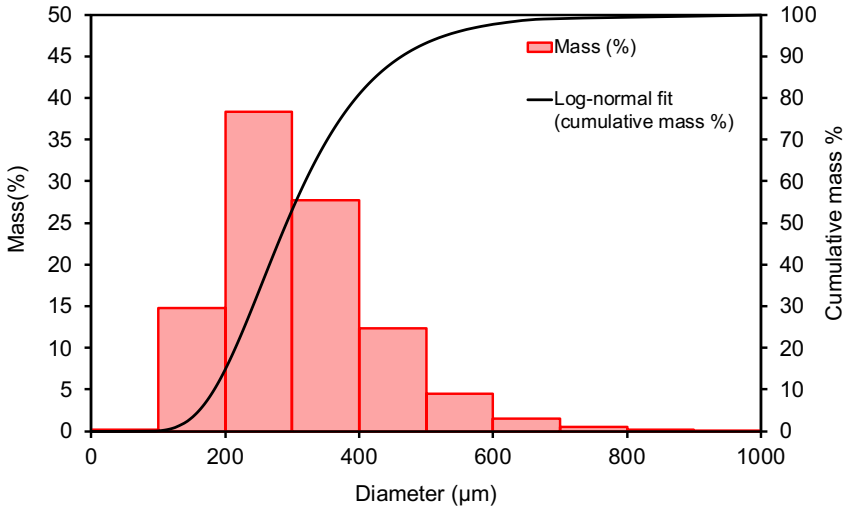

Figure 2. *Granule size distribution of the powder used*

4.1.2. INSTRUMENTED DIE USED TO CHARACTERISE THE SPRAY-DRIED POWDER

Figure 3 shows the instrumented die used in this study to characterise the mechanical properties of the powder by means of an oedometer test. Oedometer testing makes it possible to quantify both the compressibility and the deformation of a powder when a progressive vertical load is applied to it. The process consists of two stages: a loading stage, in which the vertical load is progressively increased, and an unloading stage, in which the vertical load decreases.

The die in which the test was carried out is made of carbon steel and has a lateral shank through which the radial force exerted by the powder against the die walls during pressing is transmitted. Therefore, the containment die has a cross-through hole and a radial load cell is fitted to record the pressure exerted laterally by the powder.

Using this die, it was possible to simultaneously record the axial pressure exerted on the powder and the radial pressure exerted by the powder on the die walls.

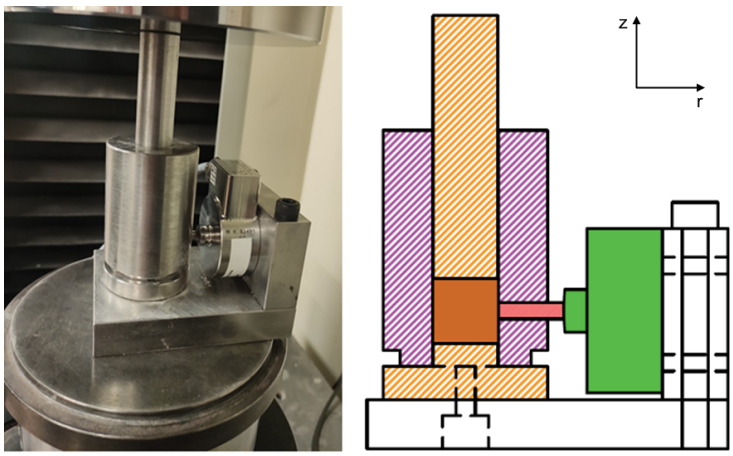

Figure 3. *Instrumented die used to calibrate the model*

4.1.3. FLOATING DIE USED TO FORM CYLINDRICAL TEST SPECIMENS

Figure 4 shows the floating die used in this study to form cylindrical specimens with which to calibrate the model. The carbon steel die comprises an upper punch to transmit the axial force of the press to the powder, and a floating containment die, connected to the base by means of springs. The purpose of this floating die is to minimise the effect of friction exerted by the die walls on the powder. This enables cylindrical specimens with an aspect ratio (height/diameter) greater than 2 and the homogeneous density required for uniaxial compression tests to be obtained.

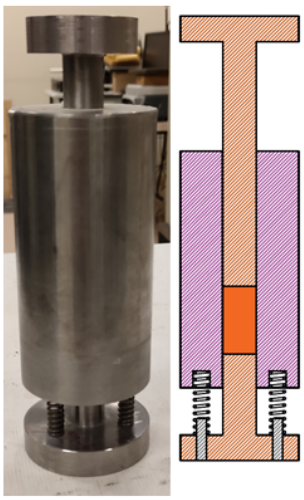

Figure 4*. Floating die used for pressing test specimens with a high aspect ratio.*

4.1.4. UNIVERSAL TEST MACHINE

An INSTRON 5889 universal test machine, shown in figure 5, was used to record the experimental data during the pressing and fracture tests. The machine had built-in 200kN load cells, both at the top and the bottom of the die, which enabled the upper and lower axial pressure exerted by the equipment on the powder and on the formed specimens to be monitored during the course of the study. In all the tests carried out, piston displacement speed was 0.035 mm/s.

Figure 5. *Instron 5889 universal test machine used in the calibration procedures.*

4.2. IDENTIFICATION OF MODEL PARAMETERS

4.2.1. SHEAR FAILURE SURFACE PARAMETERS

Shear failure surface is determined in the p-q plane by Eq (*1*), the parameters of which are ***β*** (friction angle) and ***d*** (material cohesion). Both parameters can be determined from diametral compression and uniaxial compression tests.

A diametral compression test consists of compressing a cylindrical specimen by applying force in the radial direction. The test consists of determining the radial tensile strength (σ_t) of the specimen from the maximum compressive force (reached immediately before the specimen breaks) using the following formula:

$$\sigma_t = \frac{2F_t}{\pi D h} \qquad (7)$$

where F_t represents the crushing force and D and h are the diameter and thickness of the test piece, respectively.

Uniaxial compression testing consists of also compressing a cylindrical specimen but this time, the force is applied in the axial direction. In this test, axial compressive strength (σ_c) is obtained from:

$$\sigma_c = \frac{4F_c}{\pi D^2} \qquad (8)$$

where F_c is the maximum axial compressive force (read the instant before the specimen breaks).

Once σ_t and σ_c have been obtained, it is possible to determine ***β*** and ***d*** by means of the following expressions [11]:

$$\beta = tan^{-1}\left[\frac{3(\sigma_c - \sqrt{13}\sigma_t)}{\sigma_c - 2\sigma_t}\right] \quad (9)$$

$$d = \frac{\sigma_c\sigma_t(\sqrt{13} - 2)}{\sigma_c - 2\sigma_t} \quad (10)$$

For more detailed information about the experimental procedure implemented in both tests, please see reference [12] in the bibliography.

A total of 4 uniaxial compression tests and 4 diametral compression tests were carried out using test pieces 200 mm in diameter and 8 mm and 400 mm thick, respectively. Previously, these test specimens had been formed at 4 different maximum pressures: 8, 22, 250, 500 kgf/cm^2. Given the scatter to be expected in this type of test, 3 repetitions were carried out for the uniaxial compression test and 10 for the diametral compression test.

4.2.2. "CAP" YIELD SURFACE PARAMETERS

To define the "cap" yield surface, 4 parameters need to be determined: ***R*** (eccentricity), $\boldsymbol{p_a}$ (evolution pressure), $\boldsymbol{p_b}$ (hydrostatic yield pressure) and ***α*** (transition region). Variable ***α*** usually lies between 0.01 and 0.05: in this study, it was set at 0.03. The other parameters can be calculated from an oedometer test during powder bed compression using the following expressions [13]:

$$R = \sqrt{\frac{2(1 + \alpha - \alpha/\cos\beta)^2}{3q_0}(p - p_a)} \quad (11)$$

$$p_a = -\frac{[3q + 4d\tan\beta(1 + \alpha - \alpha/\cos\beta)^2]}{4[tan\,\beta\,(1 + \alpha - \alpha/\cos\beta)]^2} + \frac{\sqrt{9q^2 + 24dq\,tan\,\beta\,(1 + \alpha - \alpha/\cos\beta)^2 + 8(3pq + 2q^2)[tan\,\beta\,(1 + \alpha - \alpha/\cos\beta)]^2}}{4[tan\,\beta\,(1 + \alpha - \alpha/\cos\beta)]^2} \quad (12)$$

$$p_b = p_a(1 + Rtan\beta) + Rd \quad (13)$$

where the hydrostatic pressure and the Von Mises equivalent stress are determined with the following equations, taking into account that the test is carried out using a cylindrical die:

$$p = \frac{1}{3}(\sigma_z + 2\sigma_r) \quad (14)$$

$$q = |\sigma_z - \sigma_r| \quad (15)$$

where σ_z and σ_r are the radial and axial stresses exerted on the powder during the oedometer test.

The oedometer tests were carried out in duplicate and at 4 different maximum pressures: 8, 22, 250 and 500 kgf/cm^2.

4.2.3. ELASTIC PARAMETERS

Since the DPC model is isotropic and the material is assumed to follow a linear law of elasticity, only two elastic parameters, ***E*** (Young's modulus) and ***v*** (Poisson's coefficient), need to be characterised. These parameters can be obtained by oedometer testing in which their variation as a function of the bulk density of the material is determined from the axial/radial and axial stress/deformation unloading curves, respectively, using the following equations [13]:

$$\frac{d\sigma_z}{d\sigma_r} = \frac{1-\nu}{\nu} \quad (16)$$

$$\frac{d\sigma_z}{d\varepsilon_z} = \frac{E(1-\nu)}{(1+\nu)(1-2\nu)} \quad (17)$$

where $d\sigma_z$, $d\sigma_r$ and $d\varepsilon_z$ are the increases in axial and radial stress and axial deformation during unloading.

To determine the elastic parameters, the data obtained from the oedometer tests carried out to determine the yield surface "cap" were used (see Section 4.2.2).

5. RESULTS AND DISCUSSION

5.1. OBTAINMENT OF THE SHEAR FAILURE SURFACE PARAMETERS

The shear failure surface parameters were obtained with the procedure described in Section 4.2.1. Figure 6 shows the characterisation result after all the specimens prepared for uniaxial and diametral compression testing had been tested.

Figure 7 shows plots of the mechanical strength, obtained by means of equations (7) and (8) for both types of compression test, as a function of bulk density, calculated by means of dimensional analysis of the 400-mm-thick specimens and by using the mercury immersion method on the 8-mm-thick specimens. As can be seen, uniaxial mechanical strength is greater than radial strength in all cases.

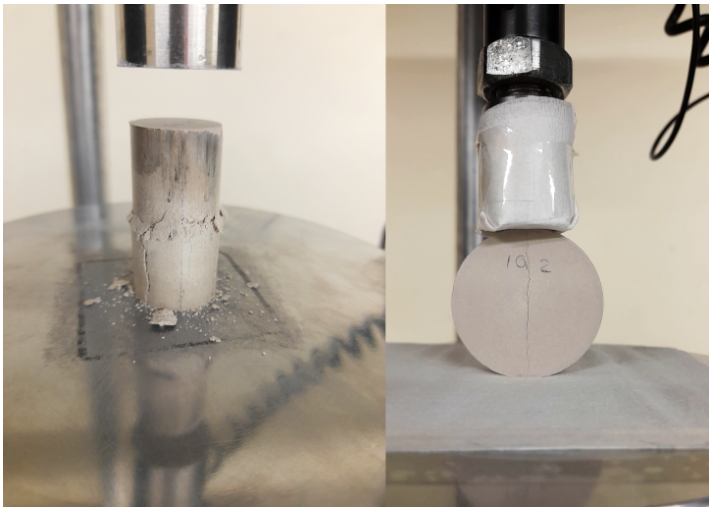

***Figure 6**. State of two porcelain tile specimens after the uniaxial compression test (left) and the diametral compression test (right).*

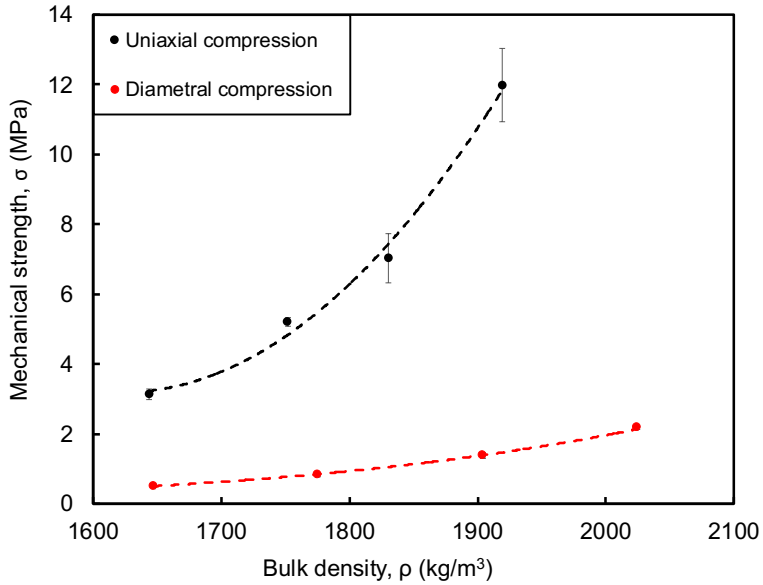

***Figure 7**. Mechanical strength of the spray-dried powder as a function bulk density, determined from uniaxial and diametral compression tests.*

5.2. OBTAINMENT OF THE "CAP" YIELD SURFACE PARAMETERS

The "cap" yield surface parameters were obtained using the procedure described in Section 4.2.2. Figure 8 shows one of the axial and radial pressure curves as a function of axial deformation from the load–unload cycle of an oedometer test with a maximum pressure of 500 kgf/cm^2.

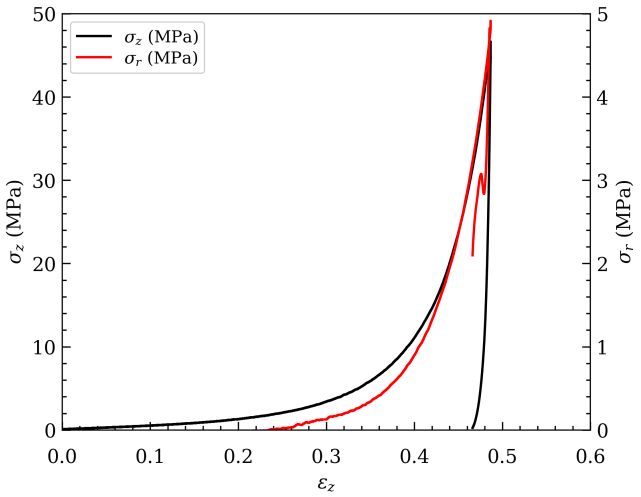

***Figure 8**. Load–unload curve obtained with the die instrumented at a maximum pressure of 500 kg$_f$/cm^2*

Note how, as displacement increases, an exponential increase can be seen in both the stress exerted on the powder and the stress exerted by the powder on the die wall. After reaching the maximum compression pressure, axial stress is relieved, which also leads to a decrease in radial pressure. This figure also reveals a small rebound in the radial stress curve during the unloading stage, which is due to the design of the instrumented die, given that the piston rod transmitting the lateral stress of the powder to the load cell jammed slightly in the cross-through hole in the die due to the effect of a small inlet of powder between the piston rod and the sleeve during pressing. However, it should be noted that this rebound does not affect the determination of the "cap" yield surface parameters.

Thus, oedometer testing can be used to determine the parameters of the "cap" yield surface with equations (11) – (15). Note that volumetric analysis enables the axial deformation of the powder (ε_z) to be related to its density. Thus, figure 9 and figure 10 show the evolution of parameters p_a, p_b and R as a function of bulk density. Note that, if an experiment with densities outside the range shown in both figures were simulated, extrapolation would be necessary.

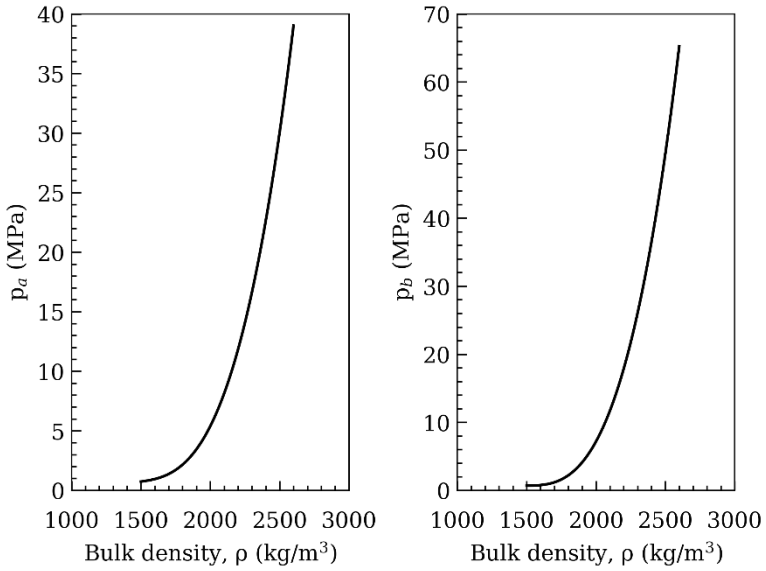

***Figure 9**. Values of parameters p_a and p_b as a function of powder bulk density.*

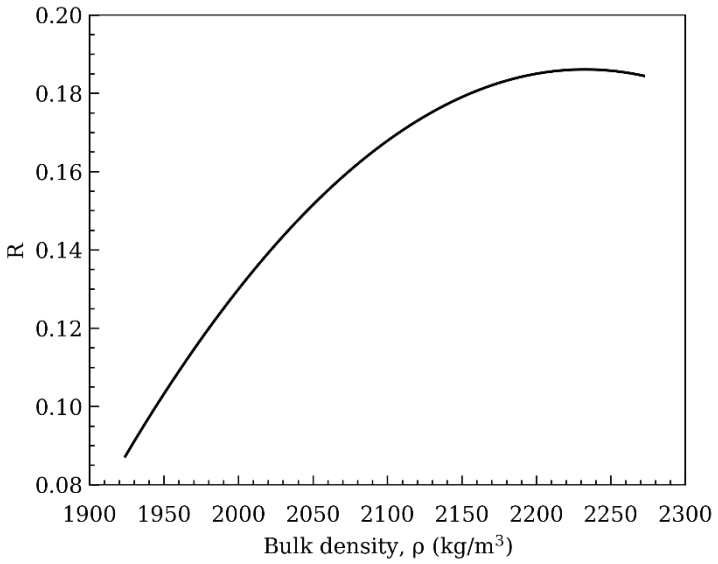

***Figure 10.** Values of parameter R as a function of powder bulk density.*

5.3. OBTAINMENT OF THE ELASTIC PARAMETERS

The elastic parameters were determined as described in Section 4.2.3. Both Young's modulus (E) and Poisson's modulus (v) are calculated from the unloading results of an oedometer test. Due to the oscillation observed in the unloading curves as a result of the die rod slightly jamming, equations (16) and (17) must only be used in the unloading range prior to rebound to determine the elastic parameters.

Figure 11 shows how the elastic parameters, obtained for each of the 4 oedometer tests performed in duplicate, evolve as a function of bulk density. Note that the bulk density for each pair of elastic parameters corresponds to the highest bulk density reached in the oedometer test. The figure shows that the higher the powder bulk density, the greater the error in predicting its elastic parameters. With respect to Poisson's modulus, such low values (<0.1) are unexpected in all cases, which is attributed to the low radial pressure exerted by the powder on the die (see figure 8).

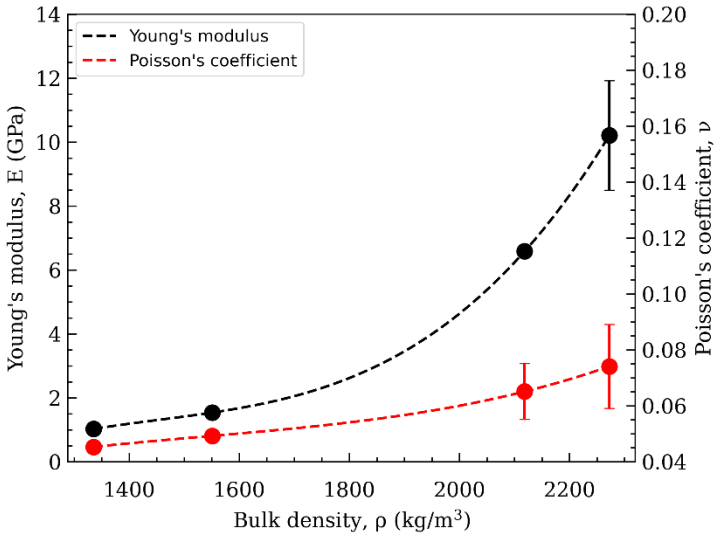

Figure 11. *Values for the elastic parameters (E,v) as a function of powder bulk density*

6. CONCLUSIONS AND FUTURE WORK

In this study, a modified Drucker–Prager Cap (DPC) model has been calibrated to predict the behaviour of a bed of spray-dried porcelain stoneware tile powder during forming. Two specific dies were designed and built for the calibration process: an instrumented die to record the axial and radial pressure exerted by the powder during an oedometer test, and a floating die to form homogeneous specimens with a high aspect ratio (height/diameter). Using diametral and uniaxial compression tests, the radial and axial tensile strength of the material was determined as a function of its bulk density, which made it possible to define the material's shear failure surface. Furthermore, by means of oedometer tests, the compression yield surface and elastic parameters of the material were obtained. The results show that the yield surfaces can be correctly defined as a function of bulk density in the higher density range, which implies the need to extrapolate the data in the lower density range. On the other hand, the unloading process during the oedometer testing could not be fully reproduced, as the piston rod used to determine radial pressure jammed slightly. Finally, once the DPC model had been calibrated, it was possible to use it to predict the forming process of porcelain stoneware tiles. Future work will aim to substantially improve prediction of the material's elastic parameters by enhancing the design of the instrumented die in order to be able to record the full unloading process in oedometer testing.

REFERENCES

[1] A. Bresciani and C. Ricci, "Continuous compaction of ceramic slabs with integrated fastening system," in *Proc. XIII Congreso Mundial de la Calidad del Azulejo y del Pavimento, QUALICER, Castellon*, 2014.

[2] K. Xia, "Numerical prediction of soil compaction in geotechnical engineering," *Comptes Rendus - Mec.*, vol. 342, no. 3, pp. 208–219, 2014.

[3] H. Chtourou, M. Guillot, and A. Gakwaya, "Modeling of the metal powder compaction process using the cap model. Part I. Experimental material characterization and validation," *Int. J. Solids Struct.*, vol. 39, no. 4, pp. 1059–1075, 2002.

[4] J. Bayle *et al.*, "Modeling of powder die compaction for press cycle optimization. To cite this version: HAL Id : cea-02509713 Modelling of powder die compaction for press cycle optimization," 2020.

[5] M. Zhou *et al.*, "A density-dependent modified Drucker-Prager Cap model for die compaction of Ag57.6-Cu22.4-Sn10-In10 mixed metal powders," *Powder Technol.*, vol. 305, pp. 183–196, 2017.

[6] J. Almanstötter, "A modified Drucker-Prager Cap model for finite element simulation of doped tungsten powder compaction," *Int. J. Refract. Met. Hard Mater.*, vol. 50, pp. 290–297, 2015.

[7] A. Michrafy, H. Diarra, J. A. Dodds, M. Michrafy, and L. Penazzi, "Analysis of strain stress state in roller compaction process," *Powder Technol.*, vol. 208, no. 2, pp. 417–422, 2011.

[8] H. Diarra *et al.*, "Finite Element Method (FEM) modeling of the powder compaction of cosmetic products: Comparison between simulated and experimental results," *Powder Technol.*, vol. 224, pp. 233–240, 2012.

[9] A. Michrafy, D. Ringenbacher, and P. Tchoreloff, "Modelling the compaction behaviour of powders: application to pharmaceutical powders," *Powder Technol.*, vol. 127, no. 3, pp. 257–266, 2002.

[10] I. Aydin, B. J. Briscoe, and K. Y. Sanhturk, "The internal form of compacted ceramic components: a comparison of a finite element modelling with experiment," *Powder Technol.*, vol. 89, pp. 239–254, 1996.

[11] B. Zhang, M. Jain, C. Zhao, M. Bruhis, R. Lawcock, and K. Ly, "Experimental calibration of density-dependent modified Drucker-Prager / Cap model using an instrumented cubic die for powder compact," *Powder Technol.*, vol. 204, no. 1, pp. 27–41, 2010.

[12] P. Doremus, F. Toussaint, and O. Alvain, "Simple Tests and Standard Procedure for the Characterisation of Green Compacted Powder," in *Recent Developments in Computer Modelling of Powder*, Kiev: IOS Press, 2001, p. 285.

[13] L. H. Han, J. A. Elliott, A. C. Bentham, A. Mills, G. E. Amidon, and B. C. Hancock, "A modified Drucker-Prager Cap model for die compaction simulation of pharmaceutical powders," *Int. J. Solids Struct.*, vol. 45, no. 10, pp. 3088–3106, 2008.